

Supporting Information

Influence of the catalyst surface chemistry on the electrochemical self-coupling of biomass-derived benzaldehyde into hydrobenzoin

Li Gong^{1,2}, Shiling Zhao³ Jing Yu^{1,4}, Junshan Li⁵, Jordi Arbiol^{4,8}, Tanja Kallio⁶, Mariano Calcabrini⁷, Paulina R. Martínez-Alanis^{1*}, Maria Ibáñez⁷, Andreu Cabot^{1,8*}

1*. Catalonia Institute for Energy Research – IREC Sant Adrià de Besòs, Barcelona 08930, Spain E-mail: pmartinez@irec.cat, acabot@irec.cat

2. University of Barcelona, Barcelona 08028, Spain.

3. School of Petrochemical Engineering, Lanzhou University of Technology, Lanzhou, 730050, China.

4. Catalan Institute of Nanoscience and Nanotechnology (ICN2), CSIC and BIST, Campus UAB, Bellaterra, 08193, Barcelona, Spain.

5. Institute of Advanced Study, Chengdu University, Chengdu, 610106, China

6. Department of Chemistry and Materials Science, Aalto University School of Chemical Engineering, P.O. Box 16100, FI-00076 Aalto, Finland.

7. IST Austria, Am Campus 1, Klosterneuburg, 3400 Austria

8. ICREA, Pg. Lluís Companys 23, 08010, Barcelona, Spain

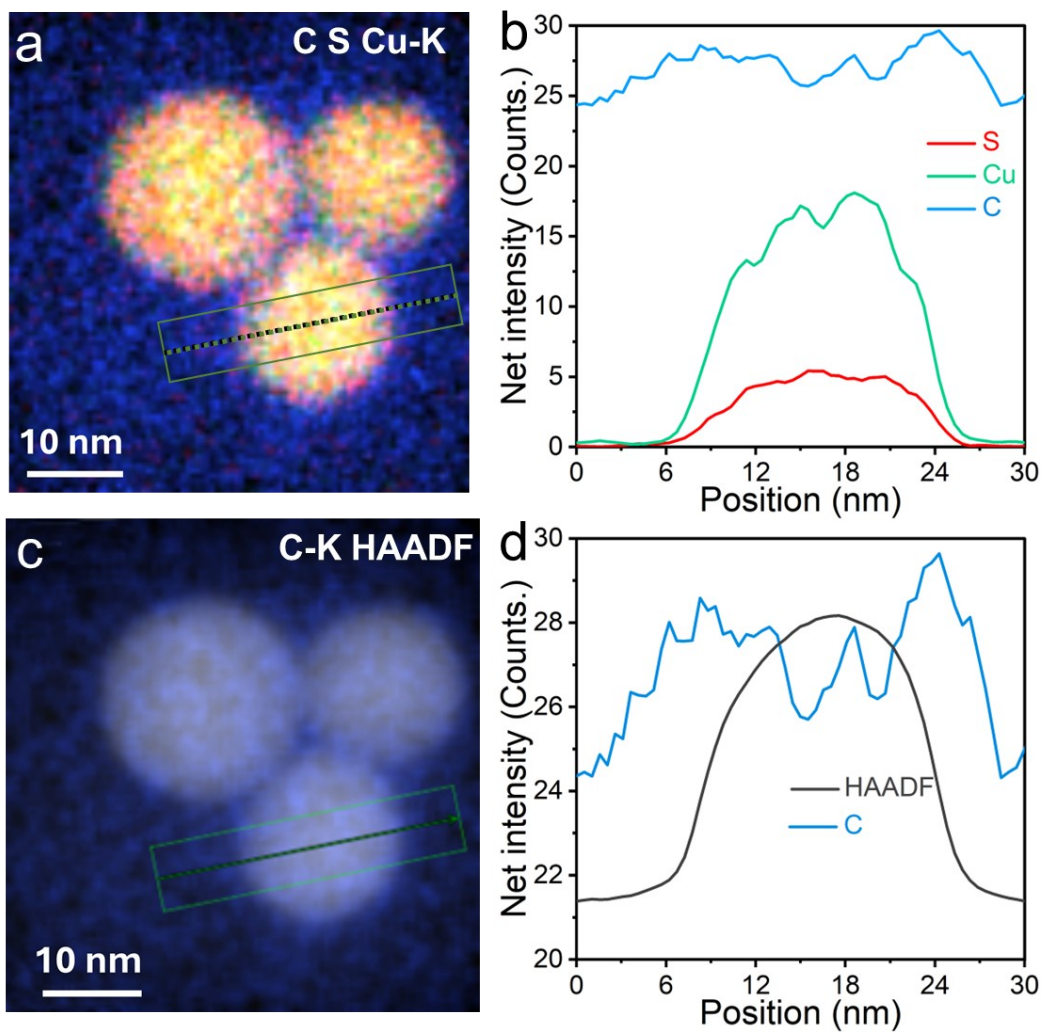


Figure S1. (a) STEM-EDS chemical composition map of different elements of Cu_2S -OAm NPs; (b) EDS linear profile of detected elements of Cu_2S -OAm NPs; (c) STEM-HAADF image of Cu_2S -OAm and element C mapping and (d) its EDS linear profile.

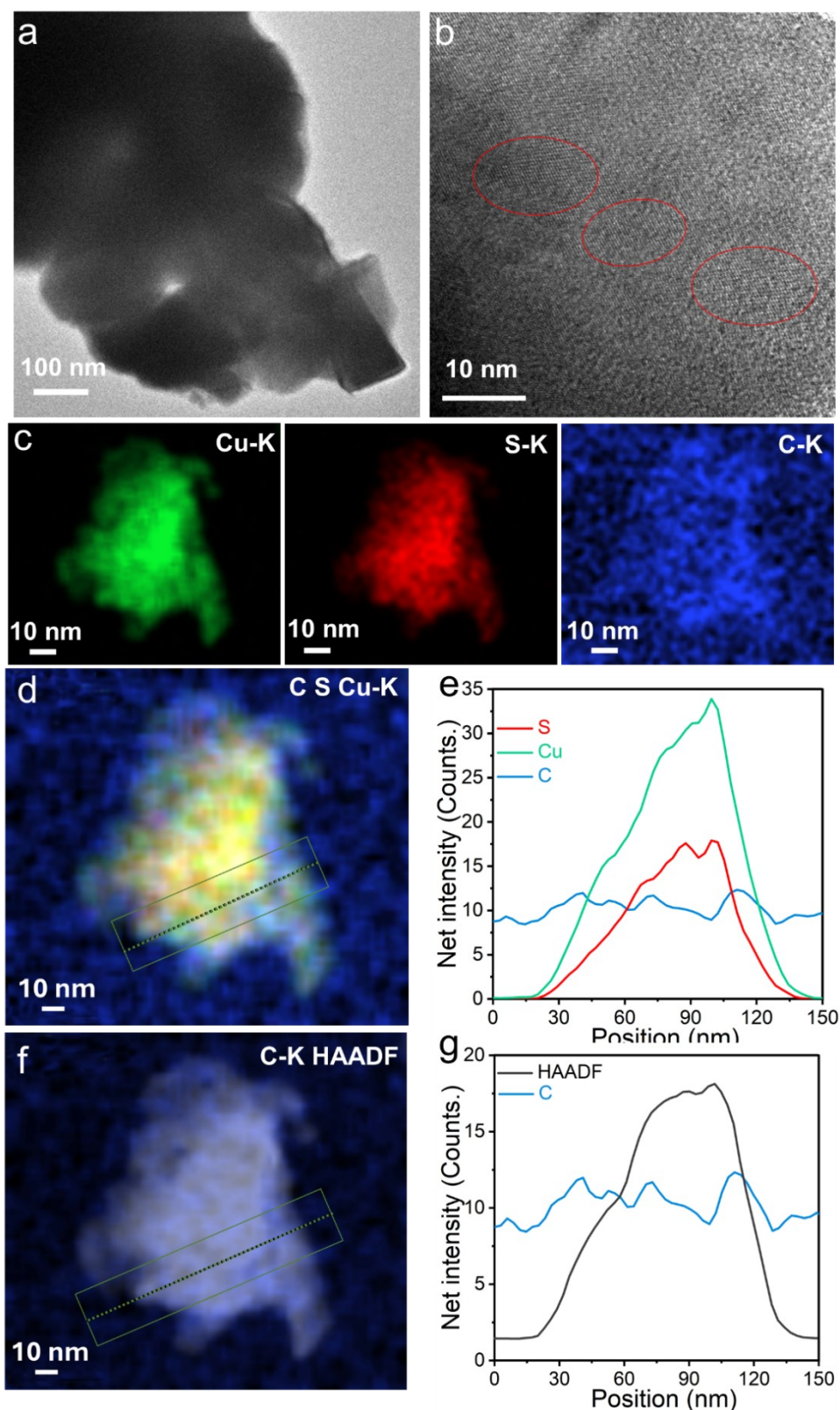


Figure S2. Structural and chemical characterization of Cu_2S . (a) TEM image; (b) High magnification TEM image; (c) STEM-EDS chemical composition maps of Cu_2S ; (d) STEM-EDS chemical composition map of different elements; (e) EDS linear profile of detected elements; (f) STEM-HAADF image of Cu_2S and element C mapping and (g) its EDS linear profile.

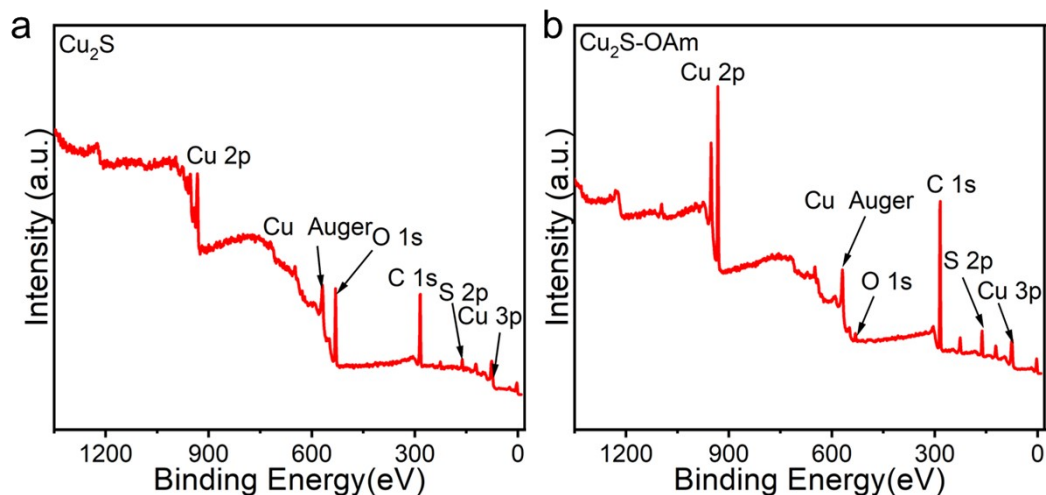


Figure S3. The XPS survey spectrum of Cu_2S and $\text{Cu}_2\text{S-OAm}$.

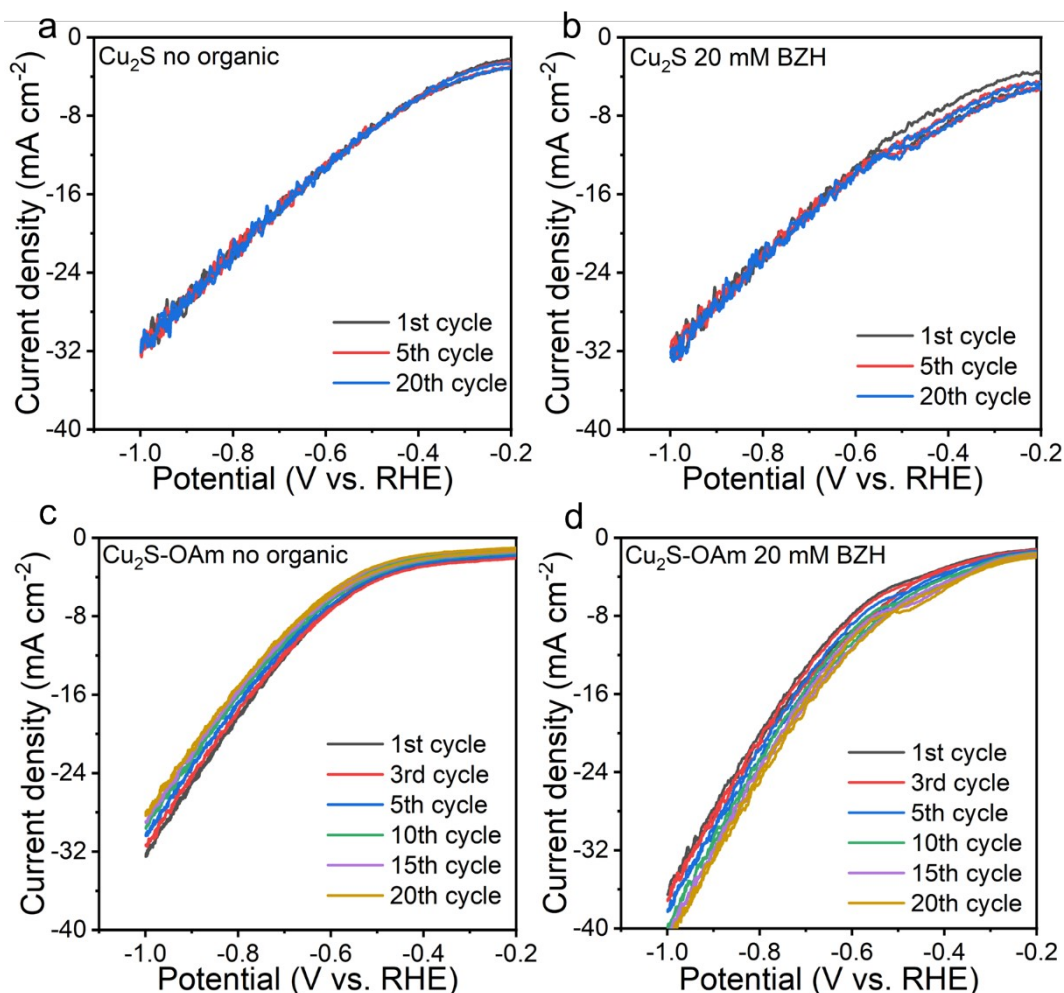


Figure S4. Stability tests using CV of (a) Cu_2S in 1 M sodium acetate-acetic acid electrolyte (pH=5.2); (b) Cu_2S in 1 M sodium acetate-acetic acid electrolyte (pH=5.2) and 20 mM BZH; (c) $\text{Cu}_2\text{S-OAm}$ in 1 M sodium acetate-acetic acid electrolyte (pH=5.2); (d) $\text{Cu}_2\text{S-OAm}$ in 1 M sodium acetate-acetic acid electrolyte (pH=5.2) and 20 mM BZH.

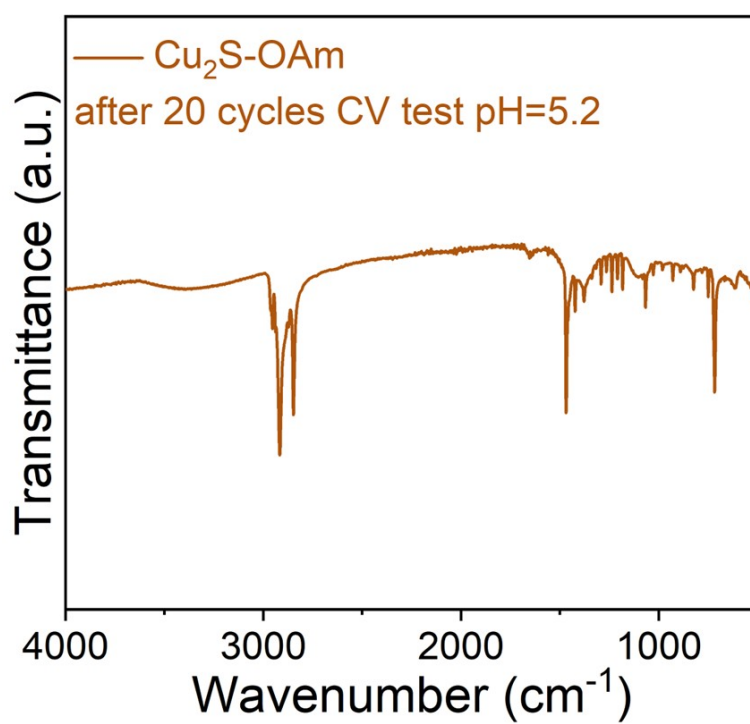


Figure S5. FTIR spectrum of Cu₂S-OAm after 20 cycles CV tests in 1 M sodium acetate-acetic acid electrolyte (pH=5.2) and 20 mM BZH.

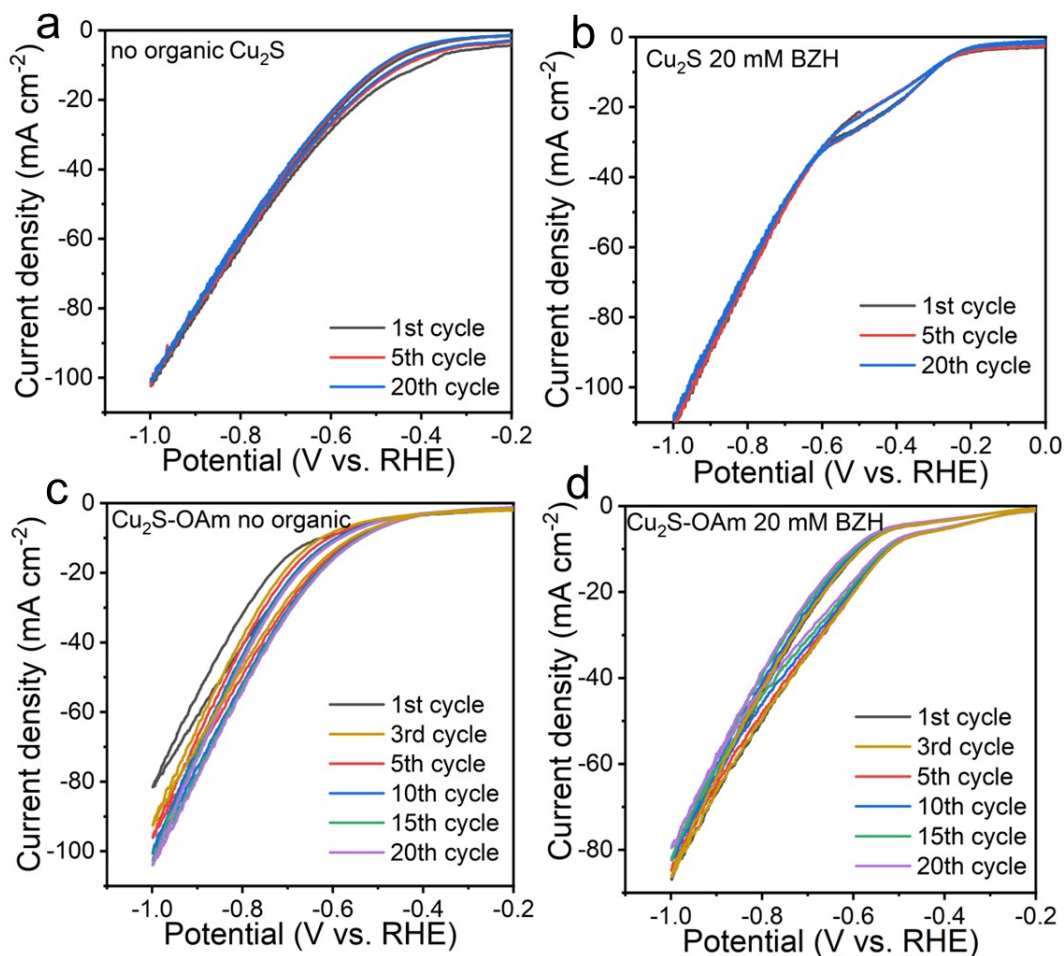


Figure S6. Stability tests of Cyclic voltammetry (CV) of (a) Cu_2S in 1 M potassium carbonate-potassium bicarbonate electrolyte (pH=9.0); (b) Cu_2S in 1 M potassium carbonate-potassium bicarbonate electrolyte (pH=9.0) and 20 mM BZH; (c) $\text{Cu}_2\text{S-OAm}$ in 1 M potassium carbonate-potassium bicarbonate electrolyte (pH=9.0); (d) $\text{Cu}_2\text{S-OAm}$ in 1 M potassium carbonate-potassium bicarbonate electrolyte (pH=9.0) and 20 mM BZH.

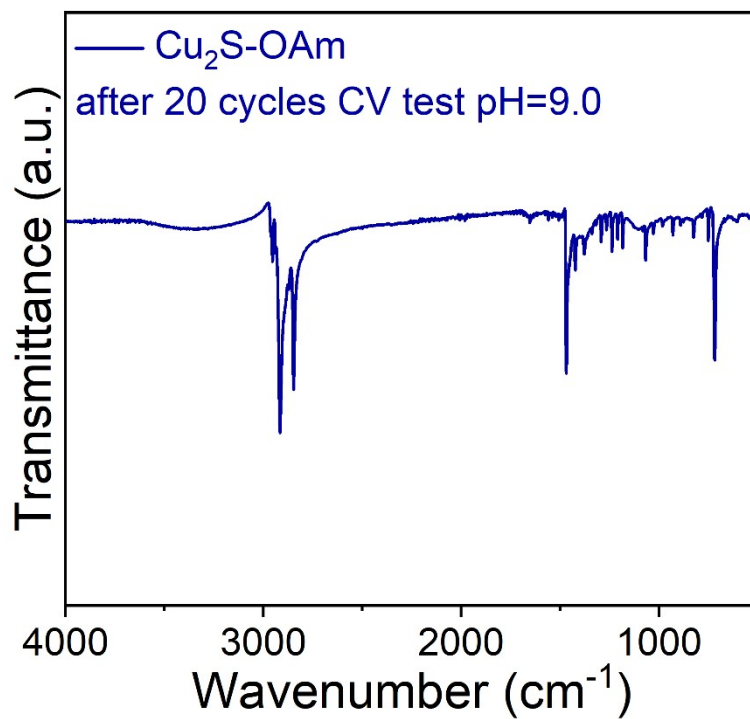


Figure S7. FTIR spectrum of Cu₂S-OAm after 20 cycles CV tests in 1 M potassium carbonate-potassium bicarbonate electrolyte (pH=9.0) and 20 mM BZH.

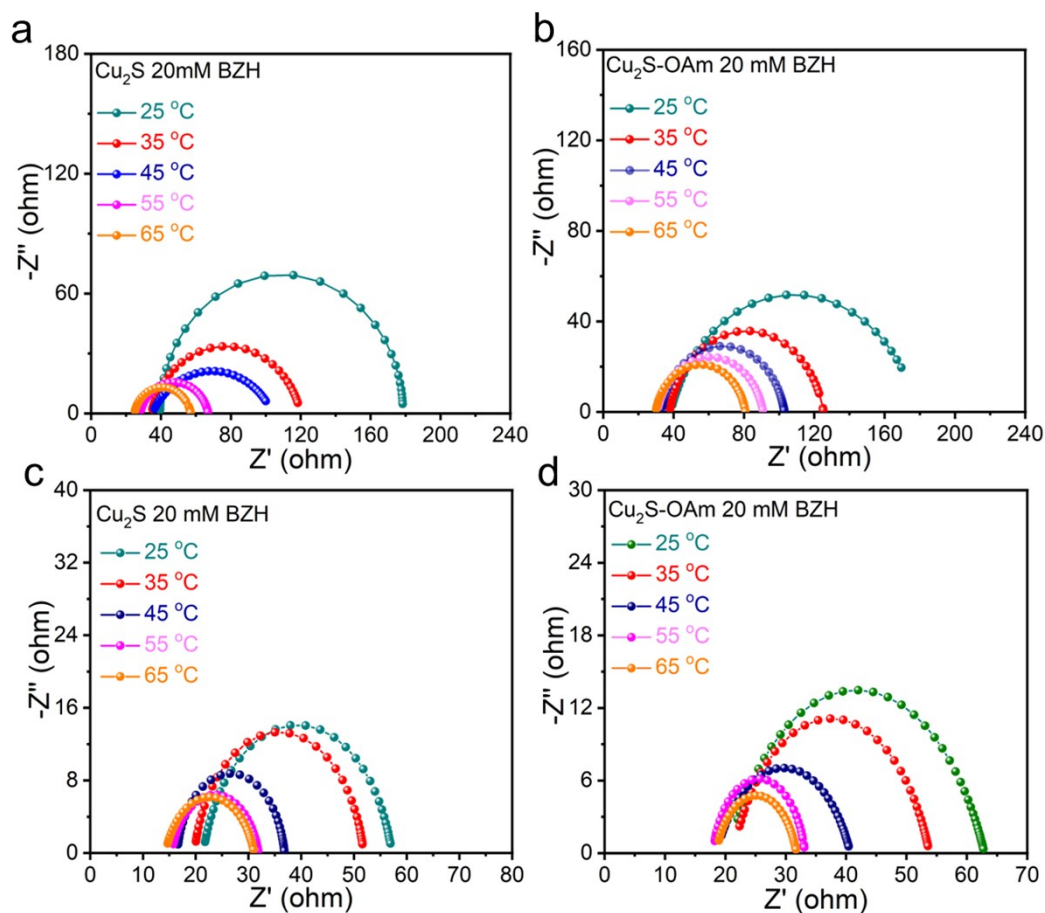


Figure S8. Nyquist plot of electrode material (a) Cu_2S ; (b) $\text{Cu}_2\text{S-OAm}$ in 1 M sodium acetate-acetic acid electrolyte (pH=5.2) and 20 mM BZH at different temperature; (c) Cu_2S ; (d) $\text{Cu}_2\text{S-OAm}$ in 1 M potassium carbonate-potassium bicarbonate electrolyte (pH=9.0) and 20 mM BZH.

Table S1. Summary of conversion of BZH at constant voltage -0.8 V vs. RHE at different pH on different electrode materials. at temperature of 25 °C.

	Electrode materials	BZH concentration (mM)	BZH Conv. %	HDB sel. %	BA sel. %
pH= 5.2	Cu_2S	20	7	62	38
	Cu_2S	40	12	60	40
	$\text{Cu}_2\text{S-OAm}$	20	8	88	12
	$\text{Cu}_2\text{S-OAm}$	40	15	86	14
pH= 9.0	Cu_2S	20	31	42	58
	Cu_2S	40	39	44	56
	$\text{Cu}_2\text{S-OAm}$	20	24	75	25

	Cu ₂ S-OAm	40	30	77	23
--	-----------------------	----	----	----	----